

Magnetically Tunable Electric Dipolar Interactions of Ultracold Polar Molecules in the Quantum Ergodic Regime

Rebekah Hermsmeier¹, Ana Maria Rey², and Timur V. Tscherbul¹

¹*Department of Physics, University of Nevada, Reno, Nevada 89557, USA*

²*JILA, National Institute of Standards and Technology, and Department of Physics, University of Colorado, Boulder, Colorado 80309, USA*



(Received 15 January 2024; accepted 13 August 2024; published 1 October 2024)

By leveraging the hyperfine interaction between the rotational and nuclear spin degrees of freedom, we demonstrate extensive magnetic control over the electric dipole moments, electric dipolar interactions, and ac Stark shifts of ground-state alkali-dimer molecules such as $\text{KRb}(X^1\Sigma^+)$. The control is enabled by narrow avoided crossings and the highly ergodic character of molecular eigenstates at low magnetic fields, offering a general and robust way of continuously tuning the intermolecular electric dipolar interaction for applications in quantum simulation, quantum sensing, and dipolar spinor physics.

DOI: 10.1103/PhysRevLett.133.143403

The nearly limitless availability of quantum levels with long lifetimes, favorable coherence properties, and strong, tunable electric dipolar (ED) interactions make ultracold polar molecules a highly attractive platform for quantum science [1–16], ultracold chemistry [17,18], and precision searches of new physics beyond the standard model [4,19]. Attaining robust quantum control over molecular electric dipole moments (EDMs) and their ED interactions is key to achieving high-fidelity quantum gates [2,20] and dynamical generation of entangled states [15,16], which can be used for a wide range of applications ranging from quantum metrology [21–24] to quantum simulation [3,25–29].

Thus far, quantum control of EDMs and ED interactions of polar molecules has only been explored for internal molecular states in the high magnetic (B) field limit, where the nuclear spins are nearly completely polarized and decoupled from molecular rotation, leading to magnetic field-insensitive molecular eigenstates of the form $|NM_N\rangle|I_1M_{I_1}\rangle|I_2M_{I_2}\rangle$, where \hat{N} is the rotational angular momentum of the molecule with eigenvalue $\sqrt{N(N+1)}$, \hat{I}_m are the spin operators for the m th nucleus ($m = 1, 2$), and M_N and M_{I_m} are the projections of \hat{N} and \hat{I}_m on the B -field axis. As a result, in this limit, B fields cannot be used to tune the EDMs of closed-shell polar molecules (such as KRb , NaK , and NaCs), precluding magnetic control over their ED interactions. While these interactions can still be tuned using external dc and ac electric (E) fields, this type of control imposes a number of significant limitations, including undesirable field inhomogeneities and decoherence mechanisms, which have prevented most experiments from operating outside the weak E field limit. Furthermore, it is impossible to turn the ED interaction off on demand using a dc E field alone when working with superpositions of rotational states with nonzero ED coupling, such as $N = 0$

and $N = 1$ states. Thus far, this challenge has been addressed by transferring the molecules to (or from) the states coupled (decoupled) by the ED interaction [3,20], requiring additional microwave or Raman pulses.

Here, we propose a general mechanism for smoothly tuning the ED interactions between polar molecules via an external dc magnetic field. By leveraging the hyperfine interactions between the nuclear spin and rotational degrees of freedom in polar alkali dimers, we demonstrate magnetic control over their EDMs over a wide dynamic range enabled by the ergodic behavior of molecular eigenstates at low B fields. Here, we adopt the term “ergodicity” in the context used in theory of quantum chaos [30–32]. Under this context, an ergodic quantum system is one that displays level repulsion quantified by a Wigner-Dyson distribution of nearest-neighbor energy level spacings and a high degree of delocalization in Hilbert space. Such criteria have been used to diagnose ergodicity-breaking transitions in C_{60} molecules [33]. Unlike previous work [23,28], our proposal does not require strong magnetic fields and/or microwave (mw) dressing, and can be realized with molecules remaining in a single quantum state, thus obviating the need for coherent state transfer to switch the ED interaction on and off [2,20]. Our results thus demonstrate the possibility of on-demand generation and tuning of ED interactions in ultracold molecular gases using dc magnetic fields alone.

We start by considering the energy level spectrum of an alkali dimer molecule (e.g., KRb) in its ground electronic and vibrational states described by the Hamiltonian [34]

$$\hat{H}_{\text{mol}} = \hat{H}_{\text{rot}} + \hat{H}_{\text{hf}} + \hat{H}_Z + \hat{H}_S, \quad (1)$$

where $\hat{H}_{\text{rot}} = B_e \hat{N}^2$ is the rotational Hamiltonian, \hat{N} is the rotational angular momentum operator, and B_e is

the rotational constant. The Stark Hamiltonian $\hat{H}_S = -\hat{d}_0 E$ [35] describes the interaction of the z component of the EDM $\hat{d}_z = \hat{d}_0$ with a dc electric field directed along a space-fixed (SF) z axis. The interaction of the molecule with an external magnetic field $B = |\mathbf{B}|$, parallel to the E field, is given by $\hat{H}_Z = -g_N \mu_N \hat{N}_z B - \sum_{m=1,2} g_{I_m} \mu_N \hat{I}_{mz} B (1 - \sigma_m)$, where g_N is the rotational g factor, g_{I_m} is the g factor for the m th nucleus, μ_N is the nuclear Bohr magneton, and σ_m are the shielding factors. The hyperfine Hamiltonian \hat{H}_{hf}

$$c_3 \hat{\mathbf{I}}_1 \cdot \hat{\mathbf{I}}_2 + \sum_{m,p} (-1)^p C_p^2(\theta, \phi) \frac{\sqrt{6}(eqQ)_m}{4I_m(2I_m - 1)} T_{-p}^2(\hat{\mathbf{I}}_m, \hat{\mathbf{I}}_m), \quad (2)$$

is dominated by the scalar spin-spin interaction $c_3 \hat{\mathbf{I}}_1 \cdot \hat{\mathbf{I}}_2$ and the nuclear electric quadrupole (NEQ) interaction [34,36]. The latter arises from the nonspherical shape of the $I \geq 1$ nuclei in KRB leading to nonzero NEQ moments, which interact with the (nonspherical) electron charge distribution inside the molecule. The interaction energy depends on the orientation of the NEQ ellipsoid (whose axis of symmetry coincides with the direction of \mathbf{I}_m) with respect to the molecular axis \mathbf{r} [37]. Transforming this electrostatic interaction to the SF frame, one obtains the second term in Eq. (2), where $C_p^k(\theta, \phi)$ is a renormalized spherical harmonic, θ and ϕ specify the orientation of \mathbf{r} in the SF frame [38], $(eqQ)_m$ are the NEQ interaction constants, and $T^2(\hat{\mathbf{I}}_m, \hat{\mathbf{I}}_m)$ is the second-rank tensor product of $\hat{\mathbf{I}}_m$ with itself [36]. The NEQ interaction couples the bare states $|NM_N, M_{I_1} M_{I_2}\rangle$ with $|N - N'| \leq 2$ and $|M_N - M'_N| \leq 2$ [28] but vanishes in the $N = 0$ manifold. As a result, in the previously underexplored low B -field regime of interest here, the eigenstates in the $N = 1$ manifold contain contributions from many bare states with different M_N, M_{I_1} , and M_{I_2} .

Figure 1 shows the energy levels and transition EDMs of KRB as a function of magnetic field at $E = 0$ obtained by exact diagonalization of the Hamiltonian (1) [23,28]. We label the levels in the order of increasing energy (with $|1\rangle$ being the ground state). The nuclear spins of ^{40}K and ^{87}Rb are $I_1 = 4$ and $I_2 = 3/2$, giving rise to $(2I_1 + 1)(2I_2 + 1)(2N + 1)$ or 36 (108) Zeeman sublevels in the $N = 0$ ($N = 1$) rotational manifolds [34]. The total angular momentum projection along the applied electromagnetic fields, $M_F = M_N + M_{I_1} + M_{I_2}$, where $\hat{\mathbf{F}} = \hat{\mathbf{N}} + \hat{\mathbf{I}}$ ($\hat{\mathbf{I}} = \hat{\mathbf{I}}_1 + \hat{\mathbf{I}}_2$) is conserved in parallel E and B fields, so only a smaller subset of levels (3 for $N = 0$ and 9 for $N = 1$) occurs in the $M_F = 7/2$ symmetry sector [34,39]. In the $N = 0$ manifold at $B \leq 20$ G, the scalar spin-spin interaction splits the energy levels into four manifolds $F = \{11/2, 9/2, 7/2, 5/2\}$ according to the value of the total angular momentum F ,

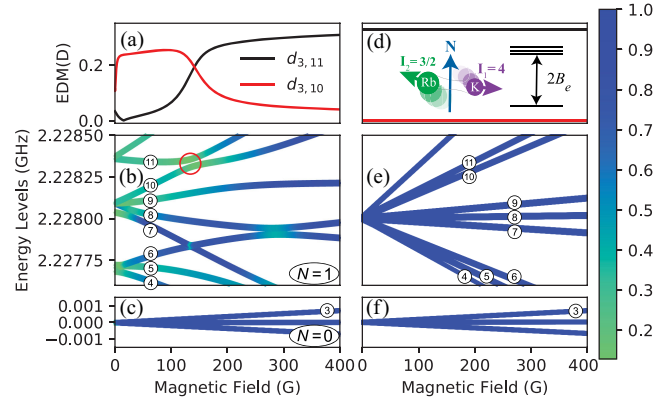


FIG. 1. (a) Representative transition EDMs $d_{3,10}$ and $d_{3,11}$ of $^{40}\text{K}^{87}\text{Rb}$ plotted as a function of magnetic field at zero electric field for $M_F = 7/2$. The $N = 1$ and $N = 0$ hyperfine Zeeman energy levels of KRB are shown in panels (b) and (c). The color of the i th energy level (see encircled labels) corresponds to the IPR ergodicity measure, $P_\alpha(i|i) = \sum_{a=1}^D |c_{\alpha i}|^4$, of the energy eigenstate $|i\rangle$ [see Eq. (3) and text]. Encircled is the avoided crossing between the $N = 1$ states $|10\rangle$ and $|11\rangle$. (d)–(f) Transition EDMs and energy levels calculated with the hyperfine interactions omitted. The maximum value of $d_{3,11}^{\text{max}} = 0.33$ D achieved in the high B -field limit is shown by the horizontal black line in panel (d). The inset in panel (d) shows a schematic of the KRB molecule with its rotational ($\hat{\mathbf{N}}$) and nuclear spin ($\hat{\mathbf{I}}_m$) angular momenta and energy levels.

which ranges from $|I - N|$ to $|I + N|$. In the $N \geq 1$ manifold the dominant effect at low B fields is the NEQ interaction, which splits the energy levels by their $\hat{\mathbf{F}}_2 = \hat{\mathbf{N}} + \hat{\mathbf{I}}_2$ angular momenta values, $F_2 = 5/2, 3/2, 1/2$, where $F_2 = |I_2 - N| \leq F_2 \leq I_2 + N$. In the high B -field limit, the Zeeman interaction takes over and groups the eigenstates by the values of good quantum numbers M_N, M_{I_1} , and M_{I_2} . The dramatic effect of the hyperfine interactions on the energy levels becomes clear when comparing Figs. 1(b) and 1(e): the levels calculated with \hat{H}_{hf} (2) set to zero [Fig. 1(e)] are straight lines, which do not experience avoided crossings.

Remarkably, as shown in Fig. 1(a), the absolute magnitude of the matrix element of the EDM [35] between the molecular eigenstates $|3\rangle$ and $|11\rangle$, $d_{3,11} = |\langle 3|\hat{d}_0|11\rangle|$, increases sharply from zero to a nearly constant value with increasing B field, while $d_{3,10}$ decreases to zero. To explain these variations, we notice that there is an avoided crossing between the energy eigenstates $|10\rangle$ and $|11\rangle$ at the same field (140 G), where $d_{3,10}$ and $d_{3,11}$ swap values. The crossing causes the eigenstates to switch their dominant bare states, only one of which has nonzero transition EDM with the ground state $|3\rangle = |00, 4 - \frac{1}{2}\rangle$, which explains the switching. Indeed, to the left of the avoided crossing encircled in Fig. 1(b), $|10\rangle \simeq |10, 4 - \frac{1}{2}\rangle$ and $|11\rangle \simeq |11, 3 - \frac{1}{2}\rangle$ and thus $d_{3,10} \rightarrow \text{const}$ and $d_{3,11} \rightarrow 0$. To the right of the crossing, the bare states are swapped, and hence $d_{3,10} \rightarrow 0$ and $d_{3,11} \rightarrow \text{const}$ at large B . This tunability is ubiquitous [40].

At a more quantitative level, the B -field dependence of the EDM matrix elements can be described by expanding molecular eigenstates $|i\rangle$ in bare states $|\alpha\rangle = |NM_N, M_{I_1}, M_{I_2}\rangle$ as [40]

$$|i\rangle = \sum_{\alpha=1}^D c_{\alpha,i}(B)|\alpha\rangle, \quad (3)$$

which gives the EDM matrix elements $\langle i|\hat{d}_0|j\rangle = \sum_{\alpha,\alpha'} c_{\alpha,i}^*(B)c_{\alpha',j}(B)\delta_{M_{I_1},M_{I_1'}}\delta_{M_{I_2},M_{I_2'}}\langle NM_N|\hat{d}_0|N'M'_N\rangle$. Because the matrix elements on the right-hand side are independent of B , the magnetic tunability of the EDM originates solely from the expansion coefficients $c_{\alpha,i}(B)$.

Qualitatively, the change in the transition EDMs arises from the coupling between the bare states with different M_N . While this coupling is induced in KRB by the NEQ interaction, it can also be due to other spin-rotation interactions, such as the electron spin-rotation and anisotropic hyperfine interactions in $^2\Sigma$ molecules [36]. As a result, the $N = 1$ eigenstates become superpositions of bare basis states with different M_N . The M_N composition of molecular eigenstates is crucial to the magnetic tunability of transition EDMs. It is encoded into the expansion coefficients $\{c_i\}$ in Eq. (3), and quantified by the inverse population ratio (IPR) [30,45] $P_\alpha(i|i) = \sum_{\alpha}|c_{\alpha,i}|^4$, which characterizes the extent of quantum ergodicity of eigenstate $|i\rangle$. Ergodic behavior is signified by $P_\alpha(i|i) \simeq 3/D$ [30], where D is the total number of bare states, $|\alpha\rangle = |NM_N, M_{I_1}, M_{I_2}\rangle$ in our case [45–50]. A small value of $P_\alpha(i|i)$ therefore indicates that many different M_N values contribute to the transition EDM involving eigenstate $|i\rangle$. This is exactly what enables a high degree of magnetic tunability. In the opposite limit of $P_\alpha(i|i) \simeq 1$, M_N becomes a good quantum number, and the EDM becomes independent of B .

Figures 1(b) and 1(c) show the IPR for the lowest eigenstates of KRB as a function of magnetic field. In the high B -field limit the eigenstates consist primarily of a single bare state, so $P_\alpha(i|i) \simeq 1$. At lower B fields, the NEQ interaction causes different bare state contributions to the individual eigenstates to mix, increasing their ergodicity and lowering $P_\alpha(i|i)$. An external magnetic field orients the nuclear magnetic moments, which decouples the nuclear spins from rotational motion and makes M_N , M_{I_1} , and M_{I_2} good quantum numbers, suppressing the mixing induced by the NEQ interaction. The competition between the NEQ and Zeeman interactions determines the ergodicity of molecular eigenstates, and, in turn, magnetic tunability of transition EDMs between them.

To test whether the exquisite magnetic tunability of the EDMs in the quantum ergodic regime extends to other observables, we plot in Fig. 2 the tensor ac Stark shifts ΔE_i^{ac} of the hyperfine sublevels $|i\rangle$ induced by the optical fields used in trapping experiments [51–56]. Minimizing these shifts is crucial for achieving long coherence times of

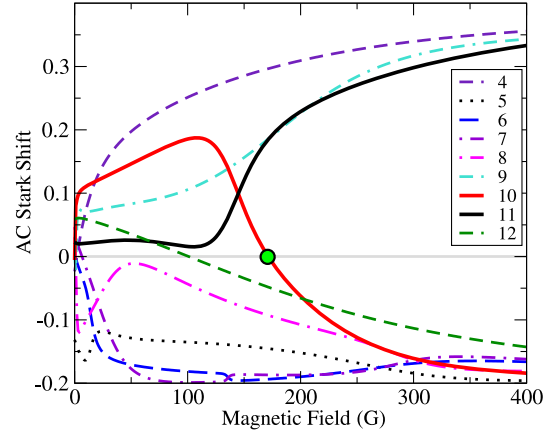


FIG. 2. Tensor ac Stark shifts, $\Delta E_i^{\text{ac}} = \langle i|P_2(\cos\theta)|i\rangle$ [28], where $P_2(\cos\theta)$ is the second-order Legendre polynomial, for the KRB states shown in Fig. 1(b) as a function of B field ($E = 0$). The green circle marks the magic B field for state $|10\rangle$.

ultracold molecules trapped in optical lattices and tweezers [3,4,7–16]. We observe that the ac Stark shifts can be efficiently controlled by applying a moderate B field. The shifts follow the same trends as those displayed by transition EDMs [see Fig. 1(a)], showing rapid variations near avoided crossings and at low B fields. Importantly, the tensor ac Stark shifts vanish at certain “magic” B fields [see Fig. 2]. This shows that, similarly to E fields [51,52], B fields can be used to prolong the coherence lifetimes of trapped alkali-dimer molecules.

Figures 3(a) and 3(d) show the magnetic field dependence of transition EDMs $d_{1,11}$ and $d_{2,12}$ in the presence of a small dc E field. In contrast to the zero E -field case, the EDMs display narrow peaks due to the additional avoided crossings seen in Figs. 3(b) and 3(e). We also observe a decrease in the ergodicity of the eigenstates compared to the field-free case. This is caused by the Stark splitting between the $M_N = 0$ and $M_N = \pm 1$ levels, which weakens the ergodicity-inducing NEQ coupling between these levels. As a result, the eigenstate composition changes more dramatically near avoided crossings than in the zero E -field case, causing rapid variations in the EDMs, as shown in Figs. 3(a) and 3(d).

We now explore magnetic control of ED interactions between two polar alkali-dimer molecules trapped in an optical lattice or a tweezer as recently demonstrated experimentally [7–16]. We encode an effective spin- $\frac{1}{2}$ system with eigenstates $|\uparrow\rangle$ and $|\downarrow\rangle$ into molecular states chosen from the hyperfine Zeeman levels in the $N = 1$ and $N = 0$ manifolds [see, e.g., Fig. 1]. The ED interaction between the molecules i and j treated as effective spin- $\frac{1}{2}$ systems may be written as [35]

$$\hat{H}_{ij} = \frac{1 - 3\cos^2\theta_{ij}}{|\mathbf{R}_{ij}|^3} \left[\frac{J_\perp}{2} (\hat{S}_+^i \hat{S}_-^j + \hat{S}_-^i \hat{S}_+^j) + J_z \hat{S}_z^i \hat{S}_z^j \right], \quad (4)$$

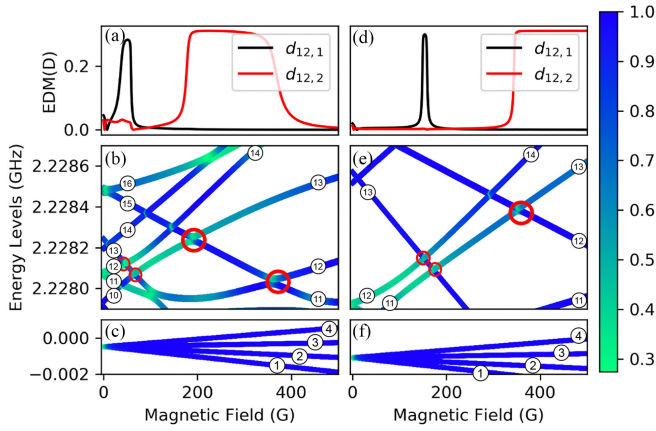


FIG. 3. Representative transition EDMs $d_{12,1}$ and $d_{12,2}$ of KRB plotted as a function of magnetic field for $M_F = -3/2$ at $E = 0.2$ kV/cm (a) and $E = 0.3$ kV/cm (d). The corresponding $N = 0$ and $N = 1$ Zeeman energy levels (see encircled labels) are shown in panels (c) and (b), respectively. The color of the energy levels corresponds to the ergodicity of molecular eigenstates. Encircled are the avoided crossings between the $N = 1$ levels responsible for the tunable behavior of the EDMs in panels (a) and (d).

where \hat{S}_\pm^i and \hat{S}_z^i are the effective spin- $\frac{1}{2}$ operators, θ_{ij} is the angle between \mathbf{E} and the vector joining the molecules \mathbf{R}_{ij} , and $J_z = (d_\uparrow - d_\downarrow)^2$ and $J_\perp = 2d_\uparrow d_\downarrow$ are the Ising and spin exchange coupling constants [28,35]. The tunability of these constants is key to generating metrologically useful many-body entangled states [23,57] and exploring new regimes of far-from-equilibrium quantum magnetism [3,29] using the XXZ Hamiltonian (4).

Figure 4 shows the magnetic field dependence of the spin exchange coupling J_\perp for several representative encodings of the effective spin- $\frac{1}{2}$ into molecular hyperfine states, such as $|\uparrow\rangle = |3\rangle$, $|\downarrow\rangle = |10\rangle$. We observe strong variations in J_\perp over a wide dynamic range (0–250 Hz) as the B field is

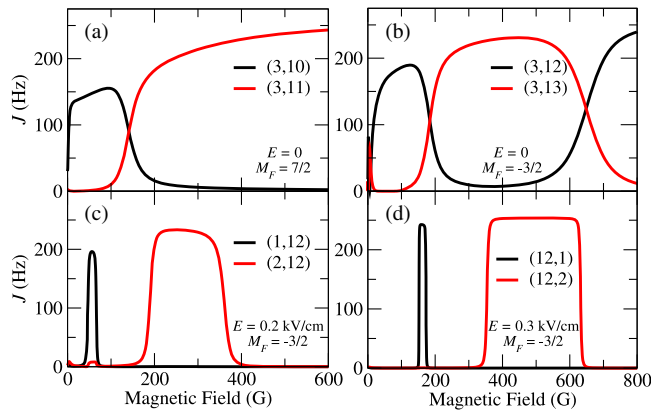


FIG. 4. Spin exchange coupling constants J_\perp plotted as a function of magnetic field at $E = 0$ for $M_F = 7/2$ (a) and $M_F = -3/2$ (b). Bottom panels show J_\perp vs B for $M_F = -3/2$ at $E = 0.2$ kV/cm (c) and 0.3 kV/cm (d).

tuned from 10 to 600 G, which match those in the transition EDMs shown in Figs. 1 and 3.

The strong dependence and fast change of J_\perp with magnetic field opens a unique opportunity to use molecules for dc magnetometry. This can be achieved by taking advantage of the so-called density shift or dipolar induced precession of the collective Bloch vector of the system in the presence of ED interactions [7,58]. The latter can be measured in a standard Ramsey spectroscopy sequence, where \mathcal{N} molecules prepared in the lowest rotational state are illuminated by a mw drive to generate a coherent superposition with a targeted excited rotational state (denoted as $|\uparrow\rangle$ state), i.e., $|\psi(0)\rangle = (\cos(\Theta)|\downarrow\rangle + \sin(\Theta)|\uparrow\rangle)^{\mathcal{N}}$. In this case the $|\uparrow\rangle$ state is the one that features the sharp resonance as a function of B . After the pulse, the system is let to evolve under the presence of ED exchange interactions for time t , accumulating a density shift, which manifests by the accumulated phase $\phi(t) = (J_z - J_\perp)\eta t \cos(\Theta)$ and $\eta = \sum_j (1 - 3\cos^2\theta_{0j})/|\mathbf{R}_{0j}|^3$. The phase is measured via a second $\pi/2$ pulse that converts it into a population difference. As any standard Ramsey sequence, the sensitivity of this protocol for an array of \mathcal{N} independent molecules is given by the standard quantum limit $\Delta\phi(t) = 1/\sqrt{\mathcal{N}}$. The fact that ϕ is a very sensitive function of B nevertheless opens a path for very precise magnetic field sensing with a sensitivity given by $\Delta B = (\sqrt{\mathcal{N}}d\phi/dB)^{-1}$ with $(d\phi/dB) = \eta t(dJ_\perp/dB)$. For unit filled molecular arrays in 2D geometries with the E field perpendicular to the molecule plane, the optimal sensitivity scales as $\Delta B = [1/\cos(\Theta)\eta\sqrt{\mathcal{N}}](dB/dJ_\perp)$, which can be as large as $\Delta B = 1/(2\eta\cos\Theta\sqrt{\mathcal{N}})$ $\mu\text{T}/\sqrt{\text{Hz}}$, close to the point of maximum slope (around $B = 152.2$ G, $(dJ_\perp/dB) \sim 200$ Hz/G). This translates into a sensitivity at the level of a few hundred pT/ $\sqrt{\text{Hz}}$ for an array of pinned 10^5 molecules assuming $\eta \sim 1$. Even though this value is at least 3 orders of magnitude less sensitive than that achievable with state of the art cold atom magnetometers [59], it potentially offers unique opportunities for improvement given the many-body nature of the shift. For example, by enhancing the range of the exchange interactions via the use of microwave cavities or by operating with itinerant arrays [7] instead of pinned particles, η could be made to scale linearly with \mathcal{N} , significantly increasing the achievable sensitivity.

Finally, our results suggest novel possibilities for high-dimensional quantum information processing [60,61] and quantum simulation [62] with ultracold polar molecules. As shown in Figs. 1 and 3, the splitting between the $N = 1$ levels near an avoided crossing can be made smaller than ≈ 50 Hz, the strength of the ED interaction at a typical lattice spacing. Molecules near such crossings can no longer be described as effective two-level systems, and the explicit inclusion of the third level becomes necessary. To this end, we describe each molecule by an effective three-level system (qutrit) comprising the ground and two

excited energy levels in the V configuration. The effective ED interaction between the V-system qutrits at the avoided crossing, where the transition EDMs are both equal to d [see Fig. 1(a)], takes the form [40]

$$\hat{H}_{ij} = |\mathbf{R}_{ij}|^{-3} d^2 (1 - 3\cos^2\theta_{ij}) [\hat{S}_x^i \hat{S}_x^j + \hat{Q}_{yz}^i \hat{Q}_{yz}^j], \quad (5)$$

where \hat{S}_α^i are the effective dipole (or spin-1) operators, and $\hat{Q}_{\alpha\beta}^i$ ($\alpha, \beta = x, y, z$) are the quadrupole operators, which form an orthogonal basis of SU(3) [63–65]. The Hamiltonian (5) contains similar processes to the ones engineered with effective all-to-all couplings in spinor quantum gases of ultracold atoms (such as four-wave mixing) [64], where spin-nematic squeezed vacuum has been experimentally realized thanks to the SU(2)-like character of the $\{\hat{S}_x, \hat{Q}_{yz}, \hat{Q}_{xz}\}$ quadratures [24]. The implementation of this Hamiltonian in dipolar molecules can open unique opportunities of realizing such states with even richer properties.

In summary, we have shown that transition EDMs of polar molecules can be magnetically tuned over a wide dynamic range, and can even be made to vanish as shown in Fig. 1(a), effectively turning a polar molecule like KRb into a nonpolar one! The underlying mechanism relies on narrow avoided crossings and the quantum ergodic behavior of molecular eigenstates. This enables continuous magnetic tuning of exchange ED interactions between zero and a maximum value without the need to transfer the molecules from one quantum state to another. Our approach requires neither strong B fields nor mw dressing, and only relies on the interplay between the hyperfine and Zeeman interactions. As a consequence, it can be applied to laser-coolable ${}^2\Sigma$ molecules [66–72] and even polyatomic molecules [33,73–79] providing a versatile tool for controlling intermolecular interactions in the quantum regime.

Acknowledgments—We are grateful for stimulating discussions with Jun Ye, James Thompson, and Nathan Prins and for feedback on the manuscript by Junyu Lin and Lee Liu. This work was supported by the NSF EPSCoR RII Track-4 Fellowship No. 1929190, the AFOSR MURI Grant No. FA9550-21-1-0069, the NSF JILA-PFC PHY-2317149, and by NIST.

[1] D. DeMille, Quantum computation with trapped polar molecules, *Phys. Rev. Lett.* **88**, 067901 (2002).
 [2] S. F. Yelin, K. Kirby, and R. Côté, Schemes for robust quantum computation with polar molecules, *Phys. Rev. A* **74**, 050301(R) (2006).
 [3] B. Yan, S. A. Moses, B. Gadway, J. P. Covey, K. R. A. Hazzard, A. M. Rey, D. S. Jin, and J. Ye, Observation of dipolar spin-exchange interactions with lattice-confined polar molecules, *Nature (London)* **501**, 521 (2013).

[4] J. L. Bohn, A. M. Rey, and J. Ye, Cold molecules: Progress in quantum engineering of chemistry and quantum matter, *Science* **357**, 1002 (2017).
 [5] V. V. Albert, J. P. Covey, and J. Preskill, Robust encoding of a qubit in a molecule, *Phys. Rev. X* **10**, 031050 (2020).
 [6] J. W. Park, Z. Z. Yan, H. Loh, S. A. Will, and M. W. Zwierlein, Second-scale nuclear spin coherence time of ultracold ${}^{23}\text{Na}{}^{40}\text{K}$ molecules, *Science* **357**, 372 (2017).
 [7] J.-R. Li, K. Matsuda, C. Miller, A. N. Carroll, W. G. Tobias, J. S. Higgins, and J. Ye, Tunable itinerant spin dynamics with polar molecules, *Nature (London)* **614**, 70 (2023).
 [8] W. G. Tobias, K. Matsuda, J.-R. Li, C. Miller, A. N. Carroll, T. Bilitewski, A. M. Rey, and J. Ye, Reactions between layer-resolved molecules mediated by dipolar spin exchange, *Science* **375**, 1299 (2022).
 [9] L. Christakis, J. S. Rosenberg, R. Raj, S. Chi, A. Morningstar, D. A. Huse, Z. Z. Yan, and W. S. Bakr, Probing site-resolved correlations in a spin system of ultracold molecules, *Nature (London)* **614**, 64 (2023).
 [10] J. T. Zhang, Y. Yu, W. B. Cairncross, K. Wang, L. R. B. Picard, J. D. Hood, Y.-W. Lin, J. M. Hutson, and K.-K. Ni, Forming a single molecule by magnetoassociation in an optical tweezer, *Phys. Rev. Lett.* **124**, 253401 (2020).
 [11] X. He, K. Wang, J. Zhuang, P. Xu, X. Gao, R. Guo, C. Sheng, M. Liu, J. Wang, J. Li, G. V. Shlyapnikov, and M. Zhan, Coherently forming a single molecule in an optical trap, *Science* **370**, 331 (2020).
 [12] W. B. Cairncross, J. T. Zhang, L. R. B. Picard, Y. Yu, K. Wang, and K.-K. Ni, Assembly of a rovibrational ground state molecule in an optical tweezer, *Phys. Rev. Lett.* **126**, 123402 (2021).
 [13] J. T. Zhang, L. R. B. Picard, W. B. Cairncross, K. Wang, Y. Yu, F. Fang, and K.-K. Ni, An optical tweezer array of ground-state polar molecules, *Quantum Sci. Technol.* **7**, 035006 (2022).
 [14] S. Burchesky, L. Anderegg, Y. Bao, S. S. Yu, E. Chae, W. Ketterle, K.-K. Ni, and J. M. Doyle, Rotational coherence times of polar molecules in optical tweezers, *Phys. Rev. Lett.* **127**, 123202 (2021).
 [15] C. M. Holland, Y. Lu, and L. W. Cheuk, On-demand entanglement of molecules in a reconfigurable optical tweezer array, *Science* **382**, 1143 (2023).
 [16] Y. Bao, S. S. Yu, L. Anderegg, E. Chae, W. Ketterle, K.-K. Ni, and J. M. Doyle, Dipolar spin-exchange and entanglement between molecules in an optical tweezer array, *Science* **382**, 1138 (2023).
 [17] R. V. Krems, Cold controlled chemistry, *Phys. Chem. Chem. Phys.* **10**, 4079 (2008).
 [18] N. Balakrishnan, Perspective: Ultracold molecules and the dawn of cold controlled chemistry, *J. Chem. Phys.* **145**, 150901 (2016).
 [19] D. DeMille, J. M. Doyle, and A. O. Sushkov, Probing the frontiers of particle physics with tabletop-scale experiments, *Science* **357**, 990 (2017).
 [20] K.-K. Ni, T. Rosenband, and D. D. Grimes, Dipolar exchange quantum logic gate with polar molecules, *Chem. Sci.* **9**, 6830 (2018).
 [21] L. Pezzè, A. Smerzi, M. K. Oberthaler, R. Schmied, and P. Treutlein, Quantum metrology with nonclassical states of atomic ensembles, *Rev. Mod. Phys.* **90**, 035005 (2018).

- [22] T. Bilitewski, L. De Marco, J.-R. Li, K. Matsuda, W. G. Tobias, G. Valtolina, J. Ye, and A. M. Rey, Dynamical generation of spin squeezing in ultracold dipolar molecules, *Phys. Rev. Lett.* **126**, 113401 (2021).
- [23] T. V. Tscherbul, J. Ye, and A. M. Rey, Robust nuclear spin entanglement via dipolar interactions in polar molecules, *Phys. Rev. Lett.* **130**, 143002 (2023).
- [24] T. Bilitewski and A. M. Rey, Manipulating growth and propagation of correlations in dipolar multilayers: From pair production to bosonic Kitaev models, *Phys. Rev. Lett.* **131**, 053001 (2023).
- [25] A. Micheli, G. K. Brennen, and P. Zoller, A toolbox for lattice-spin models with polar molecules, *Nat. Phys.* **2**, 341 (2006).
- [26] A. Micheli, G. Pupillo, H. P. Büchler, and P. Zoller, Cold polar molecules in two-dimensional traps: Tailoring interactions with external fields for novel quantum phases, *Phys. Rev. A* **76**, 043604 (2007).
- [27] L. D. Carr, D. DeMille, R. V. Krems, and J. Ye, Cold and ultracold molecules: Science, technology and applications, *New J. Phys.* **11**, 055049 (2009).
- [28] A. V. Gorshkov, S. R. Manmana, G. Chen, E. Demler, M. D. Lukin, and A. M. Rey, Quantum magnetism with polar alkali-metal dimers, *Phys. Rev. A* **84**, 033619 (2011).
- [29] K. R. A. Hazzard, S. R. Manmana, M. Foss-Feig, and A. M. Rey, Far-from-equilibrium quantum magnetism with ultracold polar molecules, *Phys. Rev. Lett.* **110**, 075301 (2013).
- [30] A. Gubin and L. F. Santos, Quantum chaos: An introduction via chains of interacting spins $1/2$, *Am. J. Phys.* **80**, 246 (2012).
- [31] F. M. Izrailev, Simple models of quantum chaos: Spectrum and eigenfunctions, *Phys. Rep.* **196**, 299 (1990).
- [32] V. Zelevinsky, B. A. Brown, N. Frazier, and M. Horoi, The nuclear shell model as a testing ground for many-body quantum chaos, *Phys. Rep.* **276**, 85 (1996).
- [33] L. R. Liu, D. Rosenberg, P. B. Changala, P. J. D. Crowley, D. J. Nesbitt, N. Y. Yao, T. V. Tscherbul, and J. Ye, Ergodicity breaking in rapidly rotating C_{60} fullerenes, *Science* **381**, 778 (2023).
- [34] J. Aldegunde, B. A. Rivington, P. S. Żuchowski, and J. M. Hutson, Hyperfine energy levels of alkali-metal dimers: Ground-state polar molecules in electric and magnetic fields, *Phys. Rev. A* **78**, 033434 (2008).
- [35] M. L. Wall, K. R. A. Hazzard, and A. M. Rey, Quantum magnetism with ultracold molecules, in *From Atomic to Mesoscale. The Role of Quantum Coherence in Systems of Various Complexities* (World Scientific, Singapore, 2015), pp. 3–37.
- [36] J. Brown and A. Carrington, *Rotational Spectroscopy of Diatomic Molecules* (Cambridge University Press, Cambridge, England, 2003).
- [37] U. Fano, Electric quadrupole coupling of the nuclear spin with the rotation of a polar diatomic molecule in an external electric field, *J. Res. Natl. Bur. Stand.* **40**, 215 (1948).
- [38] R. N. Zare, *Angular Momentum* (Wiley, New York, 1988).
- [39] J. Aldegunde, H. Ran, and J. M. Hutson, Manipulating ultracold polar molecules with microwave radiation: The influence of hyperfine structure, *Phys. Rev. A* **80**, 043410 (2009).
- [40] See Supplemental Material at <http://link.aps.org/supplemental/10.1103/PhysRevLett.133.143403> for a simple model and additional calculations of transition EDMs, and a derivation of the effective interaction between spin-1 molecular dipoles, which includes Refs. [41–44].
- [41] K. Asnaashari, R. V. Krems, and T. V. Tscherbul, General classification of qubit encodings in ultracold diatomic molecules, *J. Phys. Chem. A* **127**, 6593 (2023).
- [42] A. Zee, *Group Theory in a Nutshell for Physicists* (Princeton University Press, Princeton, NJ, 2016), Vol. 17.
- [43] J. E. Runeson and J. O. Richardson, Generalized spin mapping for quantum-classical dynamics, *J. Chem. Phys.* **152**, 084110 (2020).
- [44] C. J. Pethick and H. Smith, *Bose–Einstein condensation in Dilute Gases* (Cambridge University Press, Cambridge, England, 2008).
- [45] S. M. Pittman and E. J. Heller, The degree of ergodicity of ortho- and para-aminobenzonitrile in an electric field, *J. Phys. Chem. A* **119**, 10563 (2015).
- [46] K. S. J. Nordholm and S. A. Rice, Quantum ergodicity and vibrational relaxation in isolated molecules, *J. Chem. Phys.* **61**, 203 (1974).
- [47] T. Uzer and W. H. Miller, Theories of intramolecular vibrational energy transfer, *Phys. Rep.* **199**, 73 (1991).
- [48] R. Bigwood, M. Gruebele, D. M. Leitner, and P. G. Wolynes, The vibrational energy flow transition in organic molecules: Theory meets experiment, *Proc. Natl. Acad. Sci. U.S.A.* **95**, 5960 (1998).
- [49] D. J. Nesbitt and R. W. Field, Vibrational energy flow in highly excited molecules: Role of intramolecular vibrational redistribution, *J. Phys. Chem.* **100**, 12735 (1996).
- [50] D. M. Leitner, Quantum ergodicity and energy flow in molecules, *Adv. Phys.* **64**, 445 (2015).
- [51] S. Kotochigova and D. DeMille, Electric-field-dependent dynamic polarizability and state-insensitive conditions for optical trapping of diatomic polar molecules, *Phys. Rev. A* **82**, 063421 (2010).
- [52] B. Neyenhuis, B. Yan, S. A. Moses, J. P. Covey, A. Chotia, A. Petrov, S. Kotochigova, J. Ye, and D. S. Jin, Anisotropic polarizability of ultracold polar $^{40}\text{K}^{87}\text{Rb}$ molecules, *Phys. Rev. Lett.* **109**, 230403 (2012).
- [53] J. A. Blackmore, L. Caldwell, P. D. Gregory, E. M. Bridge, R. Sawant, J. Aldegunde, J. Mur-Petit, D. Jaksch, J. M. Hutson, B. E. Sauer, M. R. Tarbutt, and S. L. Cornish, Ultracold molecules for quantum simulation: Rotational coherences in CaF and RbCs, *Quantum Sci. Technol.* **4**, 014010 (2018).
- [54] F. Seeßelberg, X.-Y. Luo, M. Li, R. Bause, S. Kotochigova, I. Bloch, and C. Gohle, Extending rotational coherence of interacting polar molecules in a spin-decoupled magic trap, *Phys. Rev. Lett.* **121**, 253401 (2018).
- [55] P. D. Gregory, J. A. Blackmore, S. L. Bromley, J. M. Hutson, and S. L. Cornish, Robust storage qubits in ultracold polar molecules, *Nat. Phys.* **17**, 1149 (2021).
- [56] J. Lin, J. He, M. Jin, G. Chen, and D. Wang, Seconds-scale coherence on nuclear spin transitions of ultracold polar molecules in 3D optical lattices, *Phys. Rev. Lett.* **128**, 223201 (2022).

- [57] M. A. Perlin, C. Qu, and A. M. Rey, Spin squeezing with short-range spin-exchange interactions, *Phys. Rev. Lett.* **125**, 223401 (2020).
- [58] D. E. Chang, J. Ye, and M. D. Lukin, Controlling dipole-dipole frequency shifts in a lattice-based optical atomic clock, *Phys. Rev. A* **69**, 023810 (2004).
- [59] X. Bai, K. Wen, D. Peng, S. Liu, and L. Luo, Atomic magnetometers and their application in industry, *Front. Phys.* **11**, 1212368 (2023).
- [60] Y. Wang, Z. Hu, B. C. Sanders, and S. Kais, Qudits and high-dimensional quantum computing, *Front. Phys.* **8**, 589504 (2020).
- [61] R. Sawant, J. A. Blackmore, P. D. Gregory, J. Mur-Petit, D. Jaksch, J. Aldegunde, J. M. Hutson, M. R. Tarbutt, and S. L. Cornish, Ultracold polar molecules as qudits, *New J. Phys.* **22**, 013027 (2020).
- [62] D. González-Cuadra, T. V. Zache, J. Carrasco, B. Kraus, and P. Zoller, Hardware efficient quantum simulation of non-abelian gauge theories with qudits on Rydberg platforms, *Phys. Rev. Lett.* **129**, 160501 (2022).
- [63] Y. Di, Y. Wang, and H. Wei, Dipole-quadrupole decomposition of two coupled spin 1 systems, *J. Phys. A* **43**, 065303 (2010).
- [64] C. D. Hamley, C. S. Gerving, T. M. Hoang, E. M. Bookjans, and M. S. Chapman, Spin-nematic squeezed vacuum in a quantum gas, *Nat. Phys.* **8**, 305 (2012).
- [65] J. Lindon, A. Tashchilina, L. W. Cooke, and L. J. LeBlanc, Complete unitary qutrit control in ultracold atoms, *Phys. Rev. Appl.* **19**, 034089 (2023).
- [66] J. F. Barry, D. J. McCarron, E. B. Norrgard, M. H. Steinecker, and D. DeMille, Magneto-optical trapping of a diatomic molecule, *Nature (London)* **512**, 286 (2014).
- [67] S. Truppe, H. J. Williams, M. Hambach, L. Caldwell, N. J. Fitch, E. A. Hinds, B. E. Sauer, and M. R. Tarbutt, Molecules cooled below the Doppler limit, *Nat. Phys.* **13**, 1173 (2017).
- [68] H. J. Williams, S. Truppe, M. Hambach, L. Caldwell, N. J. Fitch, E. A. Hinds, B. E. Sauer, and M. R. Tarbutt, Characteristics of a magneto-optical trap of molecules, *New J. Phys.* **19**, 113035 (2017).
- [69] A. L. Collopy, S. Ding, Y. Wu, I. A. Finneran, L. Anderegg, B. L. Augenbraun, J. M. Doyle, and J. Ye, 3D magneto-optical trap of yttrium monoxide, *Phys. Rev. Lett.* **121**, 213201 (2018).
- [70] D. J. McCarron, M. H. Steinecker, Y. Zhu, and D. DeMille, Magnetic trapping of an ultracold gas of polar molecules, *Phys. Rev. Lett.* **121**, 013202 (2018).
- [71] L. Anderegg, B. L. Augenbraun, Y. Bao, S. Burchesky, L. W. Cheuk, W. Ketterle, and J. M. Doyle, Laser cooling of optically trapped molecules, *Nat. Phys.* **14**, 890 (2018).
- [72] J. J. Bureau, P. Aggarwal, K. Mehling, and J. Ye, Blue-detuned magneto-optical trap of molecules, *Phys. Rev. Lett.* **130**, 193401 (2023).
- [73] A. Prehn, M. Ibrügger, R. Glöckner, G. Rempe, and M. Zeppenfeld, Optoelectrical cooling of polar molecules to submillikelvin temperatures, *Phys. Rev. Lett.* **116**, 063005 (2016).
- [74] I. Kozyryev, L. Baum, K. Matsuda, B. L. Augenbraun, L. Anderegg, A. P. Sedlack, and J. M. Doyle, Sisyphus laser cooling of a polyatomic molecule, *Phys. Rev. Lett.* **118**, 173201 (2017).
- [75] P. B. Changala, M. L. Weichman, K. F. Lee, M. E. Fermann, and J. Ye, Rovibrational quantum state resolution of the C₆₀ fullerene, *Science* **363**, 49 (2019).
- [76] D. Mitra, N. B. Vilas, C. Hallas, L. Anderegg, B. L. Augenbraun, L. Baum, C. Miller, S. Raval, and J. M. Doyle, Direct laser cooling of a symmetric top molecule, *Science* **369**, 1366 (2020).
- [77] B. L. Augenbraun, J. M. Doyle, T. Zelevinsky, and I. Kozyryev, Molecular asymmetry and optical cycling: Laser cooling asymmetric top molecules, *Phys. Rev. X* **10**, 031022 (2020).
- [78] N. B. Vilas, C. Hallas, L. Anderegg, P. Robichaud, A. Winnicki, D. Mitra, and J. M. Doyle, Magneto-optical trapping and sub-Doppler cooling of a polyatomic molecule, *Nature (London)* **606**, 70 (2022).
- [79] C. Zhang, P. Yu, A. Jadbabaie, and N. R. Hutzler, Quantum-enhanced metrology for molecular symmetry violation using decoherence-free subspaces, *Phys. Rev. Lett.* **131**, 193602 (2023).